---

**Article:**
Mantar Gundogdu, B., Nejad, S., Gladwin, D.T. orcid.org/0000-0001-7195-5435 et al. (2 more authors) (2018) A Battery Energy Management Strategy for UK Enhanced Frequency Response and Triad Avoidance. IEEE Transactions on Industrial Electronics, 65 (12). pp. 9509-9517. ISSN 0278-0046

https://doi.org/10.1109/TIE.2018.2818642

---

# A Battery Energy Management Strategy for UK Enhanced Frequency Response and Triad Avoidance

B. Gundogdu, S. Nejad, D. T. Gladwin, M. P. Foster, and D. A. Stone

**Post Conference Paper**

**Abstract— This paper describes a control algorithm for a battery energy storage system (BESS) to deliver a charge/discharge power output in response to changes in the grid frequency constrained by the National Grid Electricity Transmission (NGET) – the primary electricity transmission network operator in the UK – whilst managing the state-of-charge (SOC) of the BESS to optimise the availability of the system. Furthermore, this paper investigates using the BESS in order to maximise Triad avoidance benefit revenues whilst layering other services. Simulation using a 2 MW/1 MWh lithium-titanate BESS validated model are carried out to explore possible scenarios using the proposed algorithms. Finally, experimental results of the 2MW/1MWh Willenhall Energy Storage System (WESS) verify the performance of the proposed algorithms.**

**Index Terms— Battery energy storage; enhanced frequency response; frequency stability; grid support; lithium-titanate; triad avoidance; Willenhall energy storage.**

## I. Introduction

With increasing environmental concerns about climate change and burning fossil fuels, and the requirement for a more sustainable grid, renewable energy sources (RES) play an essential role in energy continuity for today's electricity supply grid [1],[2]. Increased penetration of uncertain and intermittent RES on power grids causes many challenges for grid operators including increased frequency fluctuations, power quality reduction, reduced reliability and voltage transients [3]. Energy storage systems (ESSs) are one of the efficient ways to deal with such issues by decoupling energy generation from demand. Moreover, ESSs can be used to tackle the power quality concerns, especially in the UK, by providing ancillary services such as 15-minute fast frequency response, frequency regulation, Triad avoidance, load levelling and peak shaving [4], [5].

Manuscript received Month xx, 2xxx; revised Month xx, xxxx; accepted Month x, xxxx.

This work was supported in part by the UK Engineering and Physical Sciences Research Council under Grant EP/N032888/1.

Authors are with the department of Electronic and Electrical Engineering at the University of Sheffield, U.K. (emails: bmantar1@sheffield.ac.uk; shahab.nejad@sheffield.ac.uk; d.gladwin@sheffield.ac.uk; m.p.foster@sheffield.ac.uk; d.a.stone@sheffield.ac.uk)

There are various types of existing ESSs such as pumped hydro, hydrogen, fuel cells, cryogenic, compressed air, flywheel and superconducting magnetic storage [6]. In comparison to such ESSs, the battery energy storage system (BESS) has numerous advantages including faster response time compared to conventional energy generation sources, energy efficiency, storage size, long cycle life, low self-discharge rate, high charging/discharging rate capability, and low maintenance requirements [7], [8]. The cost of batteries has been decreasing in recent years and therefore there is now potential for profitable large-scale grid application. BESSs mostly participate in balancing demand and supply through frequency response services, voltage support and peak power lopping [9], [10] BESSs using various battery chemistries are installed around the world for grid support [4].

In power distribution networks, the frequency changes continuously due to the imbalance between total generation and demand; if demand surpasses generation, a decrease in the frequency will occur and vice versa [4], [11] Maintaining the grid at a nominal frequency (i.e. 50 Hz for the UK) requires the management of many disparate generation sources against varying loads. The National Grid Electricity Transmission (NGET) – the primary electricity transmission network operator in the UK – has introduced a new faster frequency response service, called Enhanced Frequency Response (EFR), to assist with maintaining the grid frequency closer to 50 Hz under normal operation [12]. A BESS is an ideal choice for delivering such a service to the power system due to its rapid response and its capability to import/export [4]. In the UK, there are limited numbers of installed BESS facilities which are suitable for providing grid support. In 2013, The UK's first grid-tie lithium-titanate BESS, the Willenhall Energy Storage System (WESS), was installed by the University of Sheffield to enable research on large scale batteries and to create a platform for research into grid ancillary services [4], [8], [13].

In the UK, the "Triad" refers to the three half-hour settlement periods with the highest system demand between the months of November and February, separated by at least ten clear days. The timing of these peaks is typically one period between 1600hrs to 1800hrs. These three periods are not known in advance and therefore are determined from the measured data analysed in March of every year. Half-hourly metered (HHM)

electricity customers in the UK pay charges proportional to their consumption during the Triad; this is called the Transmission Network Use of Service (TNUoS). The HHM customers can minimise their TNUoS charges by reducing their demand during Triad periods. Many commercial customers have an energy storage device or back-up generators to ensure the maintenance of critical supplies in case of a failure that can also be engaged to decrease Triad demand; this is known as 'Triad avoidance' [14]-[19]. It is also possible for generating assets such as BESSs to export power to the grid during the Triad, this results in a payment from the electricity supplier known as the Triad Avoidance Benefit (TAB). It is a complex task to predict the Triad periods in advance, however, many electricity suppliers offer Triad prediction services based on insufficient system margin (NISM) provided by NG and other factors such as the weather forecast [16].

Since the EFR is introduced as a new UK grid balancing service published in the late of 2016, in literature there are only a few papers about EFR service delivery for grid support. In [20], a new EFR control algorithm implemented in the DC/AC converter of a BESS was developed to fulfil the NGET EFR service requirements, however in this paper EFR control is achieved with battery energy management system rather than controlling the energy storage converter. The study [20] compares the performance of the EFR Sevice-1 (wide deadband) and Service-2 (narrow dead-band), and it was stated that the narrow service is technically more challenging, likely requiring four time the storage capacity of the wide service. That control algorithm does not cover the 15-mins frequency event control to be able to increase the availability of the BESS, especially with the narrow dead-band. However, this paper extends the basic EFR control algorithm with the two different extended 15-mins frequency event controls to achieve a maximum BESS availability for delivering EFR service. In addition, in [20], the algorithm manages the SOC of the BESS, maintaining at 49-51%. But, the SOC band should not be kept at less than 5% SOC band in order to reduce battery degradation and hence prolong its lifetime.

In [21], Cooke et al. present a method of providing the new EFR service to avoid the necessity of holding more FFR in reserve when system inertia falls. That study also introduced several alternative response curves which indicate that if arresting the fall in grid frequency in the event of a drop in generation is an important aspect of the control design, then a stepped response may provide a better service. An energy storage strategy based on PI control can help with restoration and damping of frequency. However, that response time will be slower than a stepped response so that stability can be ensured.

In [22], the authors investigate the possible performance of a BESS in EFR provision, by simulating its response to grid frequency according to the EFR service requirements, and this evaluating its ability to exchange energy for the service, a service performance indicator, and the possible aging related to battery cycling. Different EFR power versus frequency characteristics, BESS technologies and BESS energy capacities are considered in [22]. It was also assumed that the BESS are connected to the UK or to the Continental Europe (CE) synchronous area; therefore, for the CE system those requirements are adjusted according to the CE frequency behaviour. However, a major specification of the EFR service is to consider ramp-rate limits in the UK requirements, it was not considered in [22] for simplicity; power exchange rate limits internal to the batteries was also neglected. In addition, that study did not cover an extended 15-min frequency event control in order to increase the batteries availability.

In contrast to other recent works in the field; the main contribution of this paper is to present a novel control algorithm that enables BESSs to provide a bi-directional power in response to changes in the grid frequency, whilst managing the SOC of the BESS to optimise availability of the system. Moreover, this study introduces a strategy to generate additional revenues from ancillary services such as Triad Avoidance only available during the winter season.

Moreover, this paper considers layering the new UK grid frequency balancing service, EFR, with Triad Avoidance in order to maximise the system's availability and profitability. It should be noted that the previous basic study [4] presented initial three EFR control methodologies with their simulation results; and this paper extends to show how this can be used to maximise profits from other services such as Triad Avoidance. This paper also includes experimental validation with a 2MW/1MWh lithium-titanate BESS, commissioned and operated by the University of Sheffield, which is the largest research only platform for grid-tie energy storage applications.

This paper is organised as follows. In Section II, the technical specification of the new UK EFR service is described. In Section III, three different EFR service models are developed to evaluate control strategies for delivering a real-time response to deviations in the grid frequency. The first model introduces a control algorithm designed to meet the technical requirements of NGET specifications [12]. The second model addresses the EFR service design with an extended 15-minute frequency event control, in order to optimise the use of the available stored energy. The third model extends the EFR control algorithm to include a dynamic SOC target to maximise the energy stored on predicted Triad days. In Section IV the simulation results based on the 2 MW / 1 MWh BESS are analysed to verify the transient performance of the proposed control strategy. In Section V, the performance of the EFR service delivery through TAB is quantified and the performance of the proposed EFR control algorithm is verified experimentally with the 2MW / 1MWh WESS in Section VI.

## II. EFR Service Technical Specifications

EFR is introduced as a new fast frequency response service for grid balancing that can deliver full-scale active power within one second of registering a grid frequency deviation. NGET prepared an EFR specification to facilitate a tender competition for 200 MW of support provision to be distributed amongst potential energy storage providers in 2016 [12], which is described as follows.

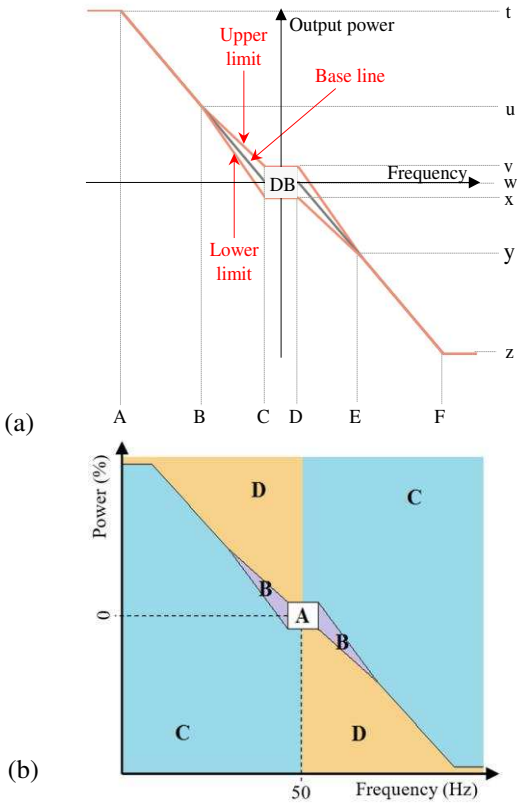


Fig. 1. NGET specifications (a) EFR envelope and (b) power zones [12].

TABLE I
EFR ENVELOPE FREQUENCY AND POWER BOUNDARIES [12]

| | Frequency (Hz) | | | Power (%) | |
|---|---|---|---|---|---|
| **Ref. Point** | **Service-1** | **Service-2** | **Ref. Point** | **Service-1** | **Service-2** |
| **A** | 49.5 | 49.5 | **t** | 100 | 100 |
| **B** | 49.75 | 49.75 | **u** | 44.44444 | 48.4536 |
| **C** | 49.95 | 49.985 | **v** | 9 | 9 |
| **D** | 50.05 | 50.015 | **w** | 0 | 0 |
| **E** | 50.25 | 50.25 | **x** | -9 | -9 |
| **F** | 50.5 | 50.5 | **y** | -44.44444 | -48.4536 |
| | | | **z** | -100 | -100 |

Energy storage providers must respond to deviations in nominal frequency (50 Hz) by decreasing or increasing their power output. Specifically, energy storage devices must provide power to the grid to respond to deviations in frequency outside of a dead band (DB). Providers must deliver continuous power to the grid as described in one of the two EFR service envelopes (Service-1, Service-2) of Table I [12]. As seen in **Error! Reference source not found.**(a), the power level must remain within the upper and lower envelopes at all times; power provided outside the envelope will decrease the service performance measurement (SPM), and thus reduce the income revenue [12]. In DB, the reference power profile is at zero MW output and hence providers do not have to respond to changes in the grid frequency. The BESS can be freely operated to charge/discharge in DB, however, the maximum export/import power must not exceed 9% of the BESS's full-scale range [12].

Providers may operate anywhere within the upper and lower envelopes to deliver a continuous service to the power system, with respect to the specified limitations on ramp rates as given in [4],[12]. For a BESS, this effectively provides some control over state-of-charge (SOC) of the battery. For the zones A, C, D in **Error! Reference source not found.**(b), the ramp rate must obey the specified values in [4], [12]. Operation in zones C and D will result in payments at a lower SPM. Hence, in such cases, EFR power output has to return to the specified envelope with respect to the ramp-rate limits given in [4]. Ramp-rate zone B is described as being the area between the upper and lower envelopes, excluding the DB, and extends to achieve the full power capability at ±0.5 Hz [12]. The allowable ramp rates within zone B depend on the rate of change of frequency. For EFR Service-1 and Service-2, the ramp rate limitations for all frequencies in zone B are shown in [4]. With these ramp limits, output power changes proportionally to changes in grid frequency, whilst allowing the energy storage providers some flexibility [12] to manage the battery SOC.

## III. EFR DESIGN ALGORITHM

A BESS model is developed in MATLAB/Simulink and verified against experimental operation of the WESS. An EFR control algorithm is then implemented on the model to deliver a grid frequency response service to the NGET specification. Fig. 2 presents the EFR control scheme implemented in EFR Model-1 [4], where the inputs are real-time grid frequency ($f$) and battery SOC, and the output is the required EFR power.

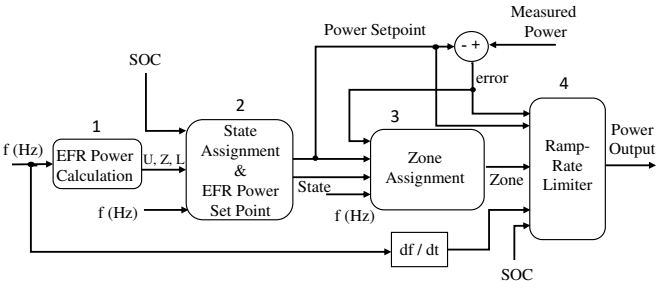


Fig. 2. EFR control scheme implemented in EFR Model-1 [4].

The algorithm starts by detecting the position of the measured grid frequency with respect to the zones bounded by vertical lines 'A' to 'F' in Fig. 1 (a). This is achieved by the 'EFR Power Calculation' block (labelled '1'), where the required EFR response envelopes are calculated. In the 2 MW BESS model, the frequency and power bounds are calculated as a function of the limits denoted in Fig. 1 (a), with their values declared in Table I. The power output is restricted to ±180 kW (i.e. 9% of 2 MW) within the DB and both services include an upper, base line and lower power line denoted $U$, $Z$ and $L$, respectively. Block 2 selects the required power line with the decision being based on the measured SOC. For example, if the current SOC is below the desired SOC range, the demanded power is calculated using the equations derived for the upper line ($U$). This has the effect of either importing energy to charge the battery or minimising the exported energy to maintain a desired SOC range. 'Zone Assignment' (Block 3) is responsible for identifying the current operating zone (refer to Fig. 1(b)) for the calculation of the power-output levels.

Finally, the change in power output per time step (1 second) for each zone is determined using the given ramp-rate limits given in [4]. In this study, battery SOC is calculated using (1) [4], where $\mathrm{SOC_{init}}$, $Q$ and $P_{\mathrm{batt}}$ represent initial SOC, Watt-hour capacity and instantaneous battery power, respectively.

$$\mathrm{SOC_{out}} = \mathrm{SOC_{init}} + \frac{\int_0^t P_{\mathrm{batt}} \cdot dt}{3600 \times Q} \quad (1)$$

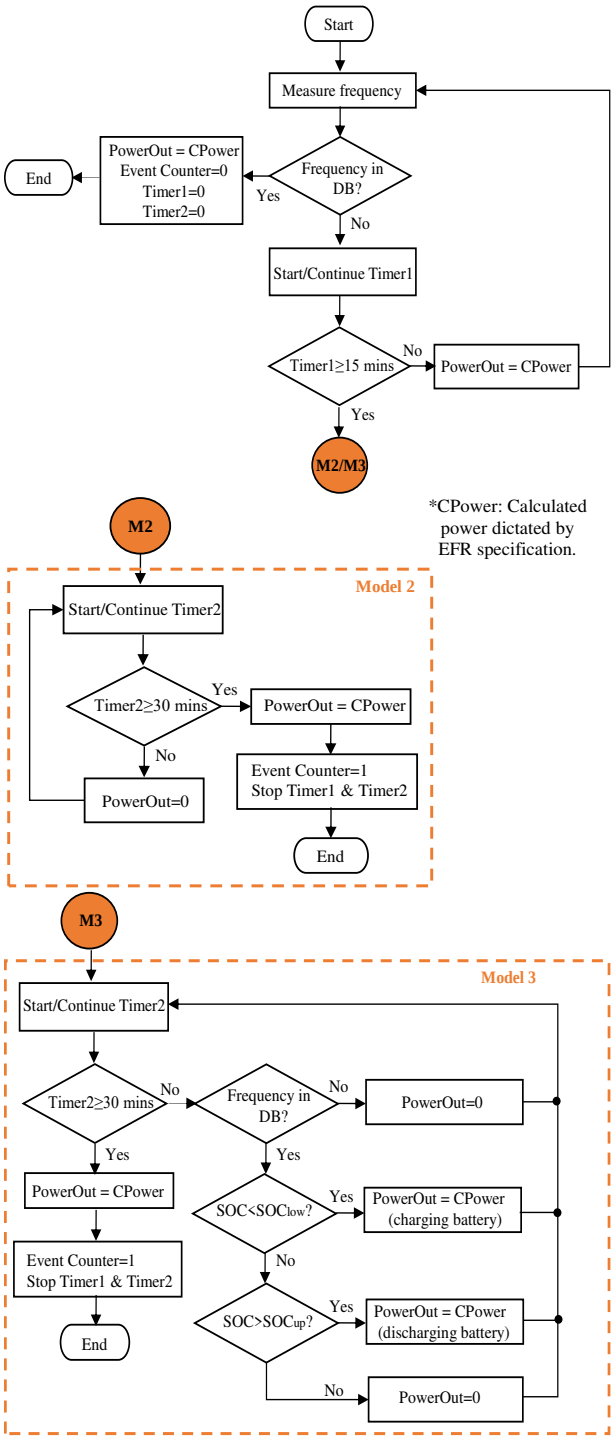


Fig. 3. Flow chart showing the structure of the two proposed battery energy management strategies for enhanced frequency response in the UK [4].

The EFR specification defines frequency outside DB for longer than 15 minutes as an extended event, whereby after the 15 minutes, it is optional to deliver power for up to 30 minutes post the grid frequency returning to DB. In order to increase the availability of the BESS in Model-1, by avoiding SOC limits, an extended 15-minute frequency event control algorithm is implemented in EFR Model-2 and Model-3, as given in Fig. 3. EFR Model-2 introduces a timed control block, which measures the length of time that the grid frequency is continuously outside of the DB. If this block measures a value higher than 15 minutes, then the BESS's output power is set to zero. The BESS remains in this state until the system frequency returns within DB, at which point a second timer starts timing for 30 minutes and the output power stays at zero until the timer expires, at which point, the EFR control is reset back to operating as EFR Model-1. EFR Model-3 allows the BESS to manage its SOC between its upper ($\mathrm{SOC_{up}}$) and lower limits ($\mathrm{SOC_{low}}$) during the 30-minute rest period by charging and discharging the battery within the ±9% power limits.

## IV. Simulation Results of EFR Models

Using a real-time frequency data set obtained from NGET [23], the three EFR models are simulated in MATLAB/Simulink. The simulation results presented in this paper are all based on a 1 MWh BESS model, which has been experimentally validated on the WESS plant in the UK, with a maximum EFR power of ±2 MW. Table V shows the parameters used in the EFR models.

### A. Simulation results of EFR Model-1

In order to show the performance of the reported EFR algorithm in Section III, the real grid frequency data for the 21st of October of 2015 [23] is employed herein, as this particular day is known to have a large period of under frequency.

TABLE I
System Parameters [12]

| Parameter | Value |
|---|---|
| Nominal frequency | 50 Hz |
| Low/high DB | ±0.015 Hz (Service-2) |
| Max/min EFR power limit | ±2 MW |
| Battery rated power/capacity | 2 MW/1 MWh |
| Battery initial SOC ($\mathrm{SOC_{init}}$) | 50% |
| SOC band ($\mathrm{SOC_{low}}$- $\mathrm{SOC_{up}}$) | 45-55% |
| Inverter efficiency ($\eta_{\mathrm{inv}}$) | 97% |
| Battery charge/discharge efficiency ($\eta_{\mathrm{C}}/\eta_{\mathrm{D}}$) | 94% |

Fig. 4 shows the simulation results of Model-1 for a 'Service-2' EFR with a target SOC band of 45-55%. On the frequency plot, the DB (±0.015 Hz) is shown by the green lines. It is clear that the SOC sharply drops, reaching 0% at 11:00, and stays there for ~30mins due to the grid frequency demands at that time. As the frequency stabilises, the EFR algorithm charges the battery when it is permissible (frequency in DB) and returns the SOC to within the specified band of 45-55%. The power response versus frequency plot of EFR Model-1 for 21st October 2015 is shown in Fig. 7(a). The red lines represent the upper, reference and lower EFR power lines. It can be seen that the EFR power (blue circles) does not remain within the required zones of 'A' and 'B'. As outlined in Fig. 1, this is

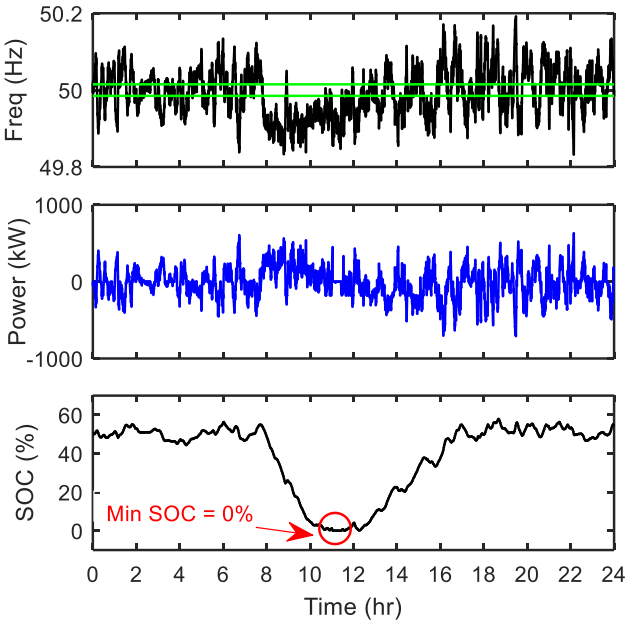


Fig. 4. Simulation results of EFR Service-2 obtained using Model-1 for 21st Oct 2015 frequency dataset.

because of the SOC reaching 0% and therefore there is no power available for delivery to the grid. This non-conformance would cause a penalty in the SPM and hence it is necessary to improve the EFR control algorithm to minimise such occurrences.

### A. Simulation Results of EFR Model-2

Model-2 introduces the extended grid frequency event timer and cuts the EFR power output after 15 minutes (Fig. 3). The same frequency data is injected into Model-2 capturing 13 15-minute extended frequency events (Fig. 5(d)). The simulation results (Fig. 5) show that the minimum battery SOC reaches 30.7% compared to 0% (Fig. 4) in Model-1. Therefore, the BESS is 100% available for providing power according to the EFR specification.

### B. Simulation Results for EFR Model-3

The EFR algorithm implemented in Model-3 allows for the charge/discharge of the battery during the 30-minute rest period (Fig. 3). The model is simulated with the 21st October 2015 grid frequency data [23] as shown in Fig. 6. The simulation results demonstrate that again, the BESS provides 100% availability as similar with Model-2 Fig. 7(b), however, the lowest SOC achieved with Model-3 is now 32.3%, compared to 30.7% (Fig. 5) of Model-2. This is a substantial achievement in terms of maximising the utilisation of the BESS stored energy.

### C. Results Analysis

In the EFR models, it is possible to define two aims for power flow in/out of the battery; the first is defined as charging and discharging the battery i.e. power is requested in either direction for the sole purpose of battery SOC management; the second is import and export which defines when the BESS is performing a mandatory response to a grid frequency event. The energy calculation of the BESS is given in (2) and (3) [5].

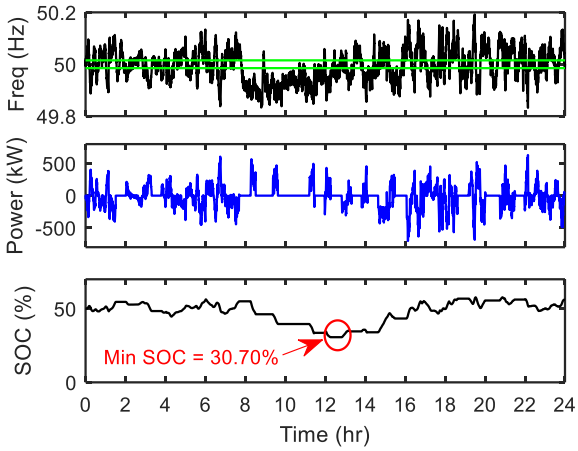


Fig. 5. Simulation results of EFR Service-2 obtained using Model-2 for 21st Oct 2015 frequency dataset.

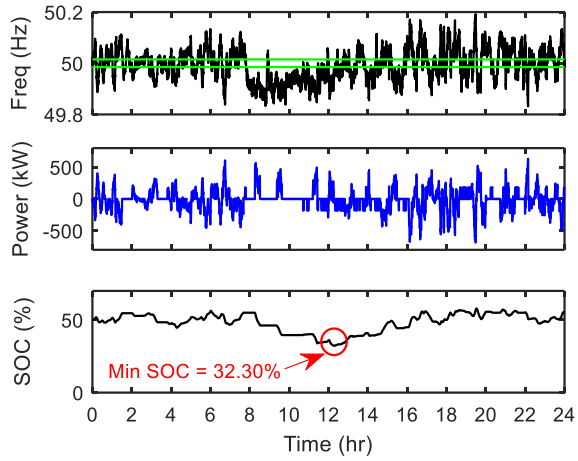


Fig. 6. Simulation results of EFR Service-2 obtained using Model-3 for 21st Oct 2015 frequency dataset.

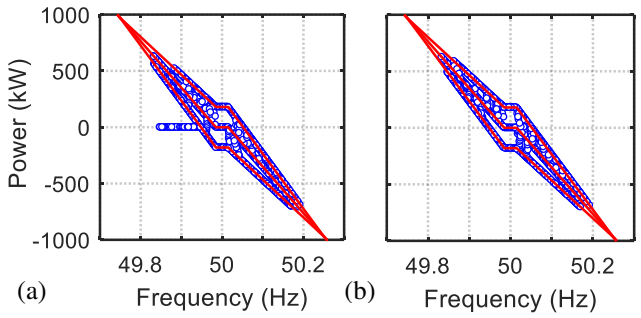


Fig. 7. EFR power response of Model-1 (a), Model-2 (b) for 21st Oct 2015.

$$\text{Discharge/Export:}\quad P > 0 \rightarrow {}^{dE}/_{dt} = -{}^{P}/_{\eta_D} \qquad (2)$$

$$\text{Charge/Import:}\quad P < 0 \rightarrow {}^{dE}/_{dt} = -P.\eta_C \qquad (3)$$

where P, E, $\eta_D$ and $\eta_C$ represent the power exchanges by the BESS, present stored energy, and battery discharging and charging efficiencies, respectively. The energy management findings of all EFR models are summarised in Table VI. It is clear that, by implementing the extended 15-minute grid frequency event control in EFR Model-2 and Model-3, the availability of the battery is increased from 98% to 100% (SPM). As desired, the battery's SOC has been shown in the simulation results to converge on the selected band of 45-55%

in all of the EFR models. In EFR Model-3, the SOC converges faster towards the desired band and it is predicted that this will minimise SOC excursions towards the limits. However, compared to EFR Model-2, this is at the expense of using more energy solely for SOC management (charge/discharge) within the DB. This is important as energy used outside of the DB (import/export) can be classified as Applicable Balancing Services Volume (ABSVD) and it is possible for this to be excluded by the energy storage provider i.e. zero cost. The difference in import/export energy observed between EFR Model-2 and Model-3 is because of the variation in SOC and so the BESS will not follow the same selection of EFR envelopes.

## V. EFR Service Delivery Through Triad Avoidance

In this section, both EFR Model-2 and Model-3 are compared for TAB using the real-time frequency dataset for the 4th December 2014, 19th January 2015, 2nd February 2015 [23-24] and 20th December 2015 [23], these represent the 2014-2015 year actual Triad days, and a high under-frequency day in 2015, respectively. The EFR service is delivered from midnight, whilst managing the SOC of the battery to within a typical range of 45-55%. The control algorithm then switches the SOC target range to 90-95% on receiving Triad warnings to maximize the available energy for delivery. Between 16:00 and 19:00 real power is exported using a weighted profile based on the statistical likelihood that a Triad would occur in each half hourly period, as shown in Table VII.

The analysis in this section considers varying the time that a Triad prediction is acted on, meaning that the SOC target is set to 90-95%, between 10:00 and 13:00. The simulation results show the SOC achieved by 16:00, with a higher SOC giving a maximum potential revenue through TAB. From Table VIII it can be seen that on 20th Dec 2015, preparing for Triad later than 12:00 is sub-optimal; a lower SOC is achieved compared to earlier times. This is because it is a particular day which has a large period of under-frequency events, as seen in Fig. 8 and Fig. 9. Preparing for Triad at 10:00, there is a considerable improvement, and it can be see that there are further gains to be made using Model-3 (87.17%) over Model-2 (70.08%).

TABLE II
ENERGY MANAGEMENT FINDINGS OF THE THREE EFR MODELS

| 21st Oct 2015 | Min SOC (%) | Max SOC (%) | SPM | Battery Charging Energy (kWh) | Battery Discharging Energy (kWh) | Battery Import Energy (kWh) | Battery Export Energy (kWh) | Total Energy (kWh) |
|---|---|---|---|---|---|---|---|---|
| **M1** | 0 | 57.96 | 0.9828 | 160.6 | 83.33 | 1744 | 1470 | 3458 |
| **M2** | 30.67 | 57.8 | 1 | 63.48 | 71.2 | 1225 | 950.5 | 2310 |
| **M3** | 32.3 | 57.93 | 1 | 136.2 | 102 | 1185 | 957 | 2381 |

TABLE III
POWER PROFILE USED FOR TRIAD AVOIDANCE

| Time (hr) | Service used for Triad | SOC band (%) | Power Delivery (kW) |
|---|---|---|---|
| 00:00 – SW | EFR | 45-55 | EFR |
| SW – 16:00 | EFR | 90-95 | EFR |
| 16:00 – 16:30 | Discharge | - | 200 |
| 16:30 – 17:30 | Discharge | - | 500 |
| 17:30 – 18:00 | Discharge | - | 300 |
| 18:00 – 18:30 | Discharge | - | 200 |
| 18:30 – 19:00 | Discharge | - | 100 |
| 19:00 – 00:00 | EFR | 45-55 | EFR |

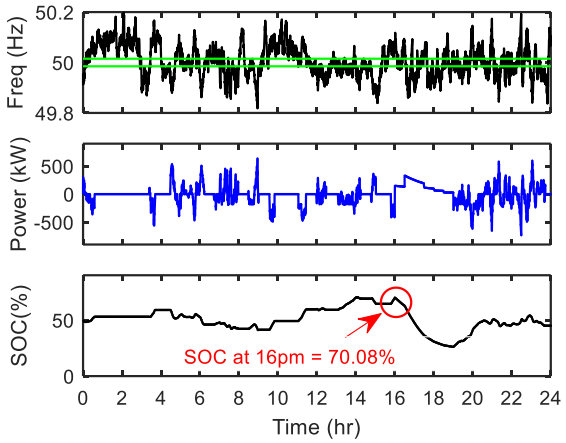


Fig. 8. Simulation results for EFR Model-2 through Triad Avoidance for 20th Dec 2015, switching mode to triad preparation at 10:00.

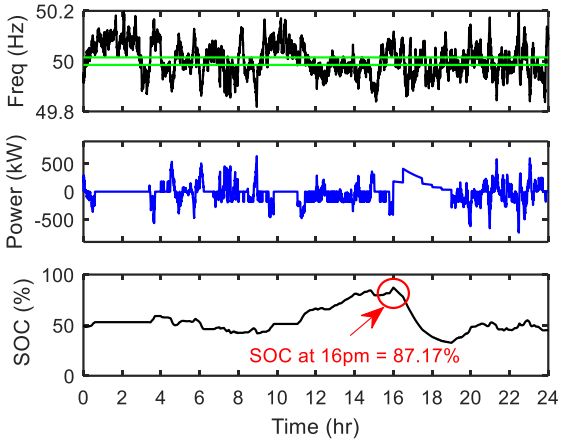


Fig. 9. Simulation results for EFR Model-3 through Triad Avoidance for 20th Dec 2015, switching mode to triad preparation at 10:00.

TABLE IV
STARTING BATTERY SOC (%) FOR TRIAD PERIOD AT 16:00

| Real/ predicted Triad days in 2015 | EFR Models used for Triad | Switch (SW) Mode to Triad Preparation at | | | |
|---|---|---|---|---|---|
| | | **10am** | **11am** | **12pm** | **13pm** |
| 4th Dec 2014 | Model-2 | 91.42 | 91.5 | 90.65 | 78.27 |
| | Model-3 | 92.23 | 91.98 | 91.5 | 79.13 |
| | **Recovery** | 0.81 | 0.48 | 0.85 | 0.86 |
| 19th Jan 2015 | Model-2 | 90 | 84.84 | 72.06 | 64.54 |
| | Model-3 | 92.43 | 86.48 | 73.61 | 66.07 |
| | **Recovery** | **2.43** | **1.64** | **1.55** | **1.53** |
| 2nd Feb 2015 | Model-2 | 99.26 | 99.26 | 99.25 | 97.79 |
| | Model-3 | 99.73 | 99.83 | 99.7 | 98.5 |
| | Recovery | 0.47 | 0.57 | 0.45 | 0.71 |
| 20th Dec 2015 | Model-2 | 70.08 | 70.08 | 63.99 | 56.57 |
| | Model-3 | 87.17 | 87.08 | 70.39 | 60.56 |
| | **Recovery** | **17.09** | **17** | **6.4** | **3.99** |

Based on the 2016 TAB payment of £45.6 / kWh [28], total triad revenues of £3229 and £2583 are obtained for Model-2 and 3 respectively (Table IX). This means that in Model-3, the

SOC converges faster (17.09%) causing the highest triad revenue (£646) as shown in Table IX, since the battery has an opportunity for charging/discharging during the 30-min rest periods, as shown by the many 15-minutes events in Fig. 9. In comparison, there is no significant SOC recovery (<2.5%) between Model-2 and Model-3 at 10:00 on the real Triad days of the year of 2014-2015 (4th Dec 2014, 2nd Feb and 19th Jan 2015) because of the low amount of extended under-frequency events.

TABLE IX
TOTAL TRIAD PROFIT (£) OBTAINED AT 17:30-18:00 PREDICTED TRIAD TIMES

| Real/ predicted Triad days in 2015 | EFR Models used for Triad | Switch (SW) Mode to Triad Preparation at | | | |
|---|---|---|---|---|---|
| | | 10am | 11am | 12pm | 13pm |
| 4th Dec 2014 | Model-2 | 3442 | 3442 | 3409 | 2934 |
| | Model-3 | 3478 | 3460 | 3442 | 2965 |
| | **Recovery** | 36 | 18 | 33 | 31 |
| 19th Jan 2015 | Model-2 | 3400 | 3193 | 2707 | 2421 |
| | Model-3 | 3490 | 3258 | 2767 | 2479 |
| | **Recovery** | **90** | **65** | **60** | **58** |
| 2nd Feb 2015 | Model-2 | 3733 | 3733 | 3730 | 3681 |
| | Model-3 | 3753 | 3753 | 3748 | 3706 |
| | Recovery | 20 | 20 | 18 | 25 |
| 20th Dec 2015 | Model-2 | 2583 | 2583 | 2353 | 2063 |
| | Model-3 | 3229 | 3223 | 2594 | 2217 |
| | **Recovery** | **646** | **640** | **241** | **154** |

## VI. EXPERIMENTAL VERIFICATIONS WITH WESS

The UK's first grid-connected lithium-titanate type of battery, WESS, was commissioned in 2015 by the University of Sheffield (UoS). The facility consists of a 1MWh, 2MW Toshiba lithium-titanate battery, interfaced to the grid through an 11 kV feed at the Willenhall Primary Substation in the UK (see Fig. 10). It aims to investigate the characteristics of a lithium-titanate type battery, as well as different battery chemistries, for providing grid support functions at scale [8], [13], [25]-[27]. The battery is made up of 40 parallel-connected racks, each consisting of 22 series-connected modules to form a rack, and each module consists of 24 cells in a 2P12S formation. There are 21,120 cells in the battery unit with a total capacity of approximately 1 MWh. The battery is connected to a four quadrant DC/AC 2 MVA converter. More technical details on the WESS can be found in [8], [13].

In order to experimentally validate the performance of the proposed EFR control algorithm, WESS was utilised as a test bed. Fig. 11 compares the results obtained from the developed EFR Model-1 and the real WESS, responding to grid frequency deviations through the EFR service for a 12-hour operation period for 21st Oct 2015. The figures show that the model is representative of the real system with a root-mean-square error (RMSE) of 0.19% and a mean-absolute-percentage error (MAPE) of 0.31% for SOC.

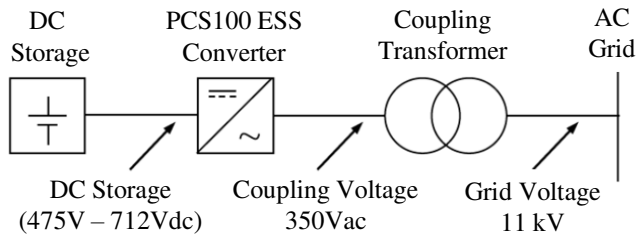


(a)


(b)

Fig. 10. (a) Block diagram and (b) photo of the 1 MWh/2MW WESS plant.

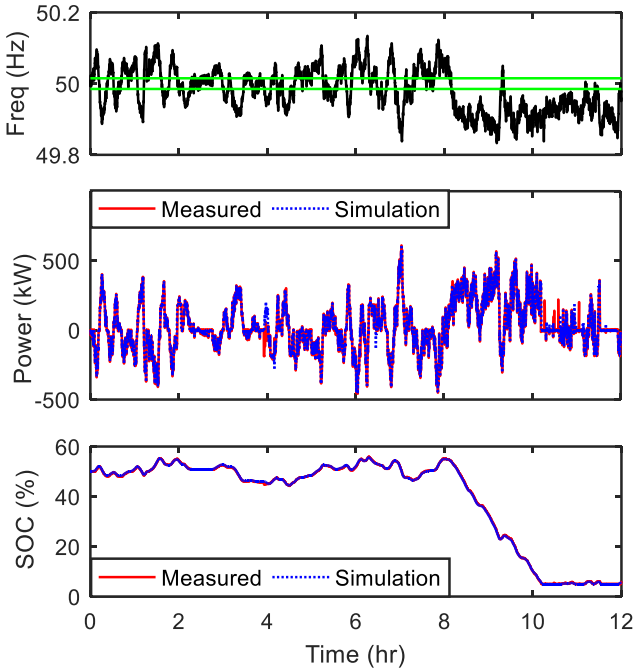


Fig. 11. Comparison of the experimental and simulation results obtained on EFR Model-1.

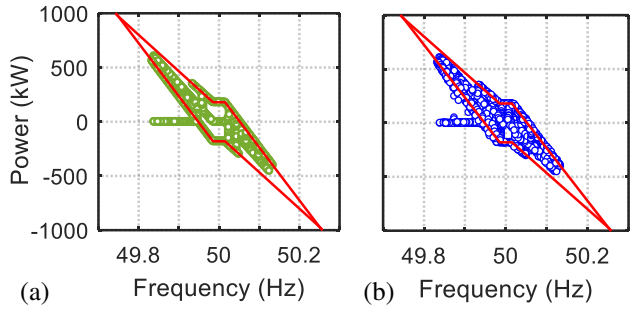


Fig. 12. EFR power versus frequency plot for (a) simulation and (b) measured using Model-1.

The slight variances in power are explained by a small difference in SOC at the boundaries of the SOC target band, meaning that each system will choose a different EFR envelope line to use. Small deviations can be accounted from the increased losses in the experimental system when compared to the model operating at very low power (<100kW). This is due to the operational efficiencies of the inverter being outside of its optimised operating range. It should also be noted that WESS is configured with an operational SOC band of 5-95%. Fig. 12 presents the delivery envelope of the proposed control algorithm for both simulation and experimental using Model-1. The comparison of experimental and model findings indicates that the proposed EFR control algorithm shows a good performance with <4.5% and ~0.3% of MAPE power and battery SOC for the 12-hour period in 21st Oct.

## VII. Conclusion

In this paper, three novel EFR control algorithms, based on the model of a 2 MW/ 1 MWh BESS, have been developed to respond to changes in the grid's frequency with a proportionate active power output. Simulation results demonstrated that all three algorithms met the UK's NGET EFR requirements, whilst managing the battery's SOC by converging towards a desired band of 45-55%. It was shown that, for the historical dataset considered, the basic EFR algorithm, Model-1, would not be able to manage the extended 15-minute grid frequency events, thus, causing the battery's SOC to drop to 0%, which would incur a service performance penalty charge. EFR Model-2 has demonstrated that in order to increase the availability of the BESS, it is necessary to stop any EFR activity after an extended 15-minute frequency event, as allowed by the EFR specifications. The third algorithm (Model-3) was shown to have a better performance in terms of SOC management by using the 30-minute rest periods in between frequency events as a window of opportunity to move SOC towards the desired band of 45-55%. However, there was a small increase in the net energy consumed. The results were validated experimentally on a 2MW / 1MWh BESS with some small variances accounted for. Finally, it was demonstrated that with strategic management of the battery's SOC during EFR delivery the BESS could be prepared in order maximise the available energy to export for TAB. The results show that the amount of energy available to export would depend greatly on the frequency conditions of the day and the time that a decision is made to commit to preparing for TAB.

## References


[1] A. Aktas, et al., "Experimental investigation of a new smart energy management algorithm for a hybrid energy storage system in smart grid applications," Electric Power Syst. Research, vol.144, Mar. 2017, pp. 185-196.

[2] N. Li, et al., "Flexible operation of batteries in power system scheduling with renewable energy," IEEE Trans. Sustainable Energy, vol. 7, no. 2, pp. 685-696, Apr. 2016.

[3] M. Dubarry, et al., "Battery energy storage system battery durability and reliability under electric utility grid operations: Analysis of 3 years of real usage, " J. Power Sources, vol. 338, pp. 65-73, Jan. 2017,

[4] B.Gundogdu, S.Nejad, D. T. Gladwin, and D. A. Stone, "A battery energy management strategy for UK enhanced frequency response," in IEEE Int. Symp. Ind. Electron. *(ISIE'17)*, 2017, Edinburg, Scotland, pp. 1-6.

[5] W. Choi et al., "Reviews on grid-connected inverter, utility-scaled battery energy storage system, and vehicle-to-grid application - challenges and opportunities," in *IEEE Transp. Electrif. Conf. Expo. (ITEC'17)*, Chicago, IL, 2017, pp. 203-210.

[6] K. C. Divya and J. Østergaard, "Battery energy storage technology for power systems—An overview, " Electr. Power Syst. Res., vol. 79, no. 4, pp. 511–520, Apr. 2009.

[7] L. H. Saw, Y. Ye, and A. A. O. Tay, "Integration issues of lithium-ion battery into electric vehicles battery pack," J. Cleaner Production, vol. 113, pp. 1032-1045, 2016

[8] T. Feehally et al., "Battery energy storage systems for the electricity grid: UK research facilities," in IET Int. Conf. Power Electron., Mach. Drives *(PEMD'*16), Glasgow, 2016, pp. 1-6.

[9] S. Chen, et al., "Penetration rate and effectiveness studies of aggregated BESS for frequency regulation," IEEE Trans. Smart Grid, vol. 7, no. 1, pp. 167-177, Jan. 2016.

[10] X. Xu, et al., "Application and modeling of battery energy storage in power systems," CSEE J. Power and Energy Syst., vol. 2, no. 3, pp. 82-90, Sept. 2016.

[11] National Grid, "Frequency Response Service," 2016. Available [Online]: http://www2.nationalgrid.com/uk/services/balancing-services/frequency-response/.

[12] National Grid, "Enhanced Frequency Response, Invitation to tender for pre-qualified parties V2.2," 2016. Available [Online]: http://www2.nationalgrid.com/Enhanced-Frequency-Response.aspx.

[13] D. Rogers, D. Gladwin, D. Stone, D. Strickland, M. Foster, "Willenhall energy storage system: Europe's largest research-led lithium titanate battery", Engineering & Technology Reference, vol. 4, pp. 1-6, Jan. 2017.

[14] C. Mullen, P. C. Taylor, V. Thornley and N. S. Wade, "Use of standby generation for reduction of transmission network charges for half-hourly metered customers," in *Int. Universities Power Eng. Conf. (UPEC'14)*, Cluj-Napoca, 2014, pp. 1-6.

[15] S. Kelly, and M. Pollitt, "An assessment of the present and future opportunities for combined heat and power with district heating (CHP-DH) in the United Kingdom," Energy Policy, vol. 38, no. 11, pp. 6936-6945, 2010.

[16] M. Dixon, "Working with the electricity industry in times of rapid change - a telecomms user's experience," in Int. Telecommun. Energy Annu. Conf. *(INTELEC'04)*, 2004, Chicago, IL, pp.100-106.

[17] R. Turvey, "Ensuring adequate generation capacity," Utilities Policy, vol. 11, no. 2, pp. 95-102, 2003.

[18] M. G. Dixon, "Profitable use of standby generators in a competitive electricity market," in Int. Telecommun. Energy Conf. (INTELEC'99), Copenhagen, 1999, pp. 1-7.

[19] C. Mullen, N. S. Wade, O. Olabisi, and P. C. Taylor, "The impact of the coincidence of STOR and triad events on STOR provider's net-income considering load recovery characteristics," CIRED Workshop 2016, Helsinki, 2016, pp. 1-4.

[20] D.M. Greenwood, et al., "Frequency response services designed for energy storage," Applied Energy, vol. 203 , pp. 115-127, Oct. 2017.

[21] A. Cooke, D. Strickland, and K. Forkasiewicz, "Energy storage for enhanced frequency response services," in Int. Universities Power Eng. Conf. (UPEC*'17*), Heraklion, 2017, pp. 1-6.

[22] S. Canevese, et al., "Simulation of enhanced frequency response by battery storage systems: The UK versus the continental Europe system," in IEEE Int. Conf. Environment Elect. Eng. and IEEE Ind. Commercial Power Syst. Europe (EEEIC / I&CPS Europe), Milan, 2017, pp. 1-6.

[23] National Grid, "Enhanced frequency response", Available [Online]: http://www2.nationalgrid.com/Enhanced-Frequency-Response.aspx

[24] National Grid, "2014-2015 Triads" Available [Online]: http://www2.nationalgrid.com/UK/Industry-information/System-charges/Electricity-transmission/Transmission-Network-Use-of-System-Charges/Transmission-Charges-Triad-Data/

[25] National Grid, "Battery Storage Investigation Report - June 2015," Available [Online]: http://www2.nationalgrid.com/WorkArea/DownloadAsset.aspx?id=8589939031

[26] TUoS, "Giant UK battery launched to tackle challenges in energy storage Available [Online]: https://www.sheffield.ac.uk/news/nr/willenhall-battery-energy-storage-1.558968

[27] TUoS, " Willenhall: 2MW battery energy storage demonstrator Available [Online]: http://www.sheffield.ac.uk/creesa/willenhall/facts
[28] National Grid, "Transmission network use of system (TNUoS) charges" Last seen February 2018, Available [Online]: https://www.nationalgrid.com/uk/electricity/charging-and-methodology/transmission-network-use-system-tnuos-charges

**Burcu Gundogdu** was born in Istanbul, Turkey, in 1988. She received the M.Sc. degree from the Department of Electrical Engineering for Sustainable and Renewable Energy, University of Nottingham, UK, in 2014. She is currently working towards a Ph.D. degree in the Department of Electronic and Electrical Engineering, University of Sheffield, UK. Her research interests include power system analysis, energy storage systems, renewable energy systems, and design and control of power electronics.

**Shahab Nejad** was born in 1989 in Iran. He received the M.Sc. degree in Avionic Systems in 2012, and the Ph.D. degree in electronic and electrical engineering in 2016, all from the University of Sheffield, U.K. He is currently a post-doctoral researcher at the Centre for Research into Electrical Energy Storage and Applications at the University of Sheffield. His current research interests include battery management, interfacing and controlling of megawatt-scale grid-tie battery storages and second-life applications for electric vehicle batteries.

**Daniel T. Gladwin** received the M.Eng. (Hons.) degree in electronic engineering and the Ph.D. degree in automated control structure design and optimization using evolutionary computing from the University of Sheffield, Sheffield, UK. He is a Senior Lecturer in the Department of Electrical and Electronic Engineering, the University of Sheffield, with particular interest for research into energy storage and management, power electronics, and intelligent systems.

**Martin P. Foster** received the M.Sc.(Eng.) degree in control systems, and the Ph.D. degree for his thesis "Analysis and Design of High-order Resonant Power Converters" all the University of Sheffield, Sheffield, U.K., in 2000, and 2003, respectively. Since 2003, he has been a member of the academic staff in the Department of Electronic and Electrical Engineering, The University of Sheffield, with research interests including the modelling and control of switching power converters, multilevel converters and battery management.

**David A. Stone** received the B.Eng. degree in electronic engineering from the University of Sheffield, Sheffield, U.K., in 1984, and the Ph.D. degree from Liverpool University, Liverpool, U.K., in 1989. He is currently a Professor of electrical engineering with the University of Sheffield, where he has been since 1989, joining the Electrical Machines and Drives group as a member of academic staff responsible for power electronics and energy storage.